IFERC-CSC workshop on JFRS-1
June 4th, 2025
Online

Report of GGHB Project

Contents

1. Fuel supply and helium ash exhaust in flux-driven turbulence
2. Verification of global electromagnetic gyrokinetic code
3. Summary & Future plans

Kenji IMADERA

Graduate School of Energy Science, Kyoto University

Collaborators

A. Ishizawa, S. Okuda (Kyoto U.)

E. Poli, T. Görler, T. Hayward-Schneider (IPP)

Background - 1

- ✓ Establishment of a refueling method is an important issue to control nuclear fusion reactors.
- ✓ But, in DEMO-class high-temperature plasmas, a pellet injection reaches only up to 80-90% of the minor radius so that the central density peaking depends on particle pinch, making the prediction difficult.

Schematic picture of Japan-DEMO*

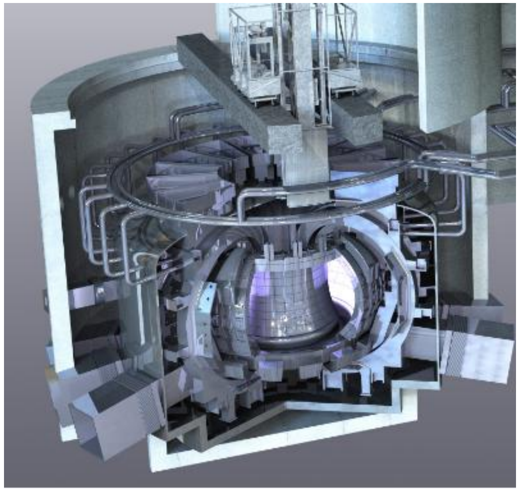

- ✓ While turbulent particle transport has been studied based on local gyrokinetic models [Angioni+, PoP-2004] , it is important to study the global physics.
- ✓ The above analysis is also meaningful to investigate impurity transport such as Helium ash exhaust.

*[https://www.fusion.qst.go.jp/rokkasyo/ddjst/]

Background - 2

<u>Radial profiles of tungsten fluxes in GYSELA full-*f* simulation</u>

[Estève+, NF-2018]

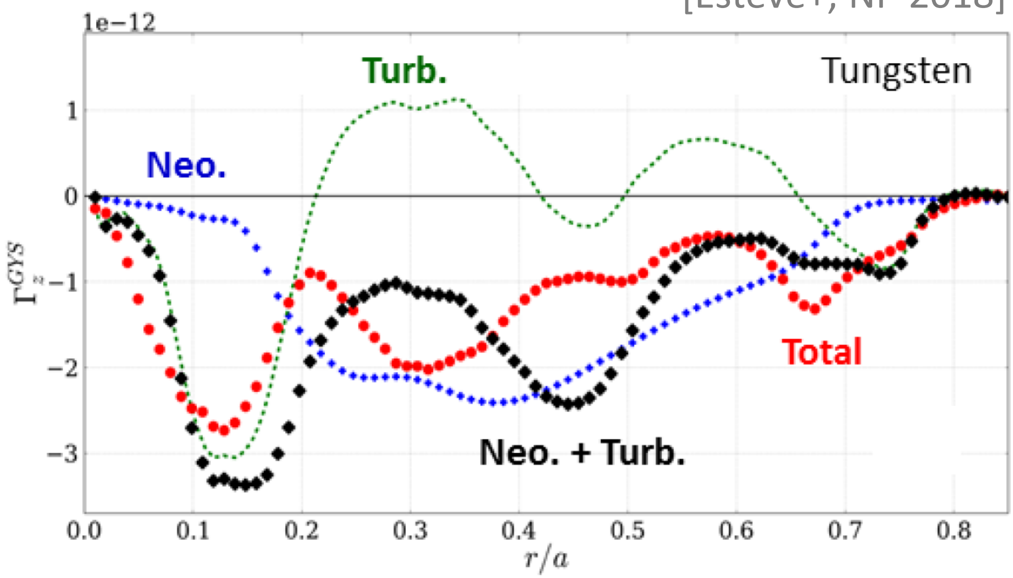

<u>Radial profiles of helium fluxes in GT5D full-*f* simulation</u>

[Idomura+, PoP-2021]

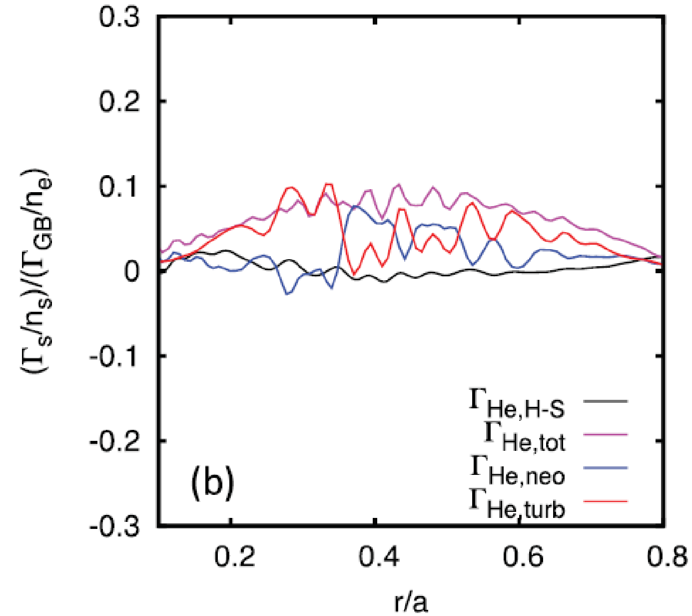

- ✓ Neoclassical and turbulent impurity transports are not additive, but have the synergy effects.
- ✓ Neoclassical flux is much larger than the theoretical estimate because of the synergy effect.

But, No full-*f* gyrokinetic simulation
from the view point of fuel supply and helium ash exhaust!

Purpose of This Work

(1) Particle transport simulation for bulk ion [Imadera+, NF-2024]

- ✓ By means of full-*f* gyrokinetic code GKNET with hybrid electron model [Imadera & Kishimoto, PPCF-2023], we investigate the effect of ion and electron heating on bulk particle transport.
- ✓ Especially, we separately discuss the contribution from (1) the E × B drift with n≠0, (2) the E × B drift with n=0, and (3) the magnetic drift.

$$\frac{dE_r}{dt} = \Gamma_{i,E\times B(n\neq 0)} + \Gamma_{i,E\times B(n=0)} + \Gamma_{i,B} - \Gamma_{e,E\times B(n\neq 0)} - \Gamma_{e,E\times B(n=0)} - \Gamma_{e,B}$$

*evaluated by gyro-center coordinate

(2) Particle transport simulation for bulk ion and helium ash [Imadera+, submitted to IAEA-2025]

- ✓ By considering helium, we also investigate the balance of fuel supply and helium ash exhaust under ion/electron heating.

(1) Governing Equations and Parameters

Governing equations

GK Boltzmann(Vlasov) equation

$$\frac{\partial}{\partial t}(\mathcal{J} f_s) + \mathcal{J}\frac{d\boldsymbol{R}}{dt}\cdot\frac{\partial f_s}{\partial \boldsymbol{R}} + \mathcal{J}\frac{dv_\parallel}{dt}\frac{\partial f_s}{\partial v_\parallel} = \mathcal{J} C_{s,s}\ (s = i, e)$$

$$\frac{d\boldsymbol{R}}{dt} = \frac{1}{B_{\parallel,s}^*}\left[v_\parallel(\boldsymbol{\nabla}\times\boldsymbol{A}) + \frac{B_0}{\Omega_s} v_\parallel^2 (\boldsymbol{\nabla}\times\boldsymbol{b}) + \frac{c}{e_s} H\,\boldsymbol{\nabla}\times\boldsymbol{b} - \frac{c}{e_s}\boldsymbol{\nabla}\times(H\boldsymbol{b})\right]$$

$$\frac{dv_\parallel}{dt} = -\frac{1}{m_s B_{\parallel,s}^*}\left[(\boldsymbol{\nabla}\times\boldsymbol{A})\cdot\boldsymbol{\nabla}H + \frac{B_0}{\Omega_s} v_\parallel \boldsymbol{\nabla}\cdot(H\boldsymbol{\nabla}\times b)\right]$$

+

GK quasi-neutrality condition

$$\frac{1}{4\pi e_i}\nabla_\perp\cdot\frac{\rho_{ti}^2}{\lambda_{Di}^2}\nabla_\perp\phi + \iint \langle \delta f_i\rangle_{\alpha,i}\frac{B_\parallel^*}{m_i} dv_\parallel d\mu = \delta n_e$$

	$(m,n) = (0,0)$	$(m,n) \neq (0,0)$
$\delta n_{e,pass}$	Kinetic	Adiabatic
$\delta n_{e,trap}$	Kinetic	Kinetic

Parameters

Parameter	Value
a_0/ρ_i	100
a_0/R_0	0.36
$(R_0/L_n)_{r=a_0/2}$	2.22
$\sqrt{m_i/m_e}$	10
ν_i^*	0.025
ν_e^*	0.025

- ✓ Hydrogen and hybrid electron are assumed
- ✓ Hereafter, we report the following two cases;

Case	R_0/L_{T_i}	R_0/L_{T_e}	Ion heating	Electron heating
(A) Ion/Electron	10	10	On	On
(B) Ion	10	6	On	Off

(1) Density Peaking/Flattening by Heating

(A) Ion/Electron

$R_0/L_{T_i} = 10$

$R_0/L_{T_e} = 10$

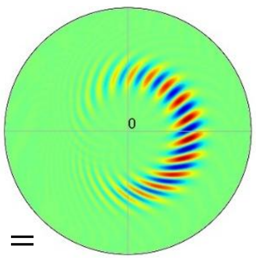

$\gamma =$ 0.62

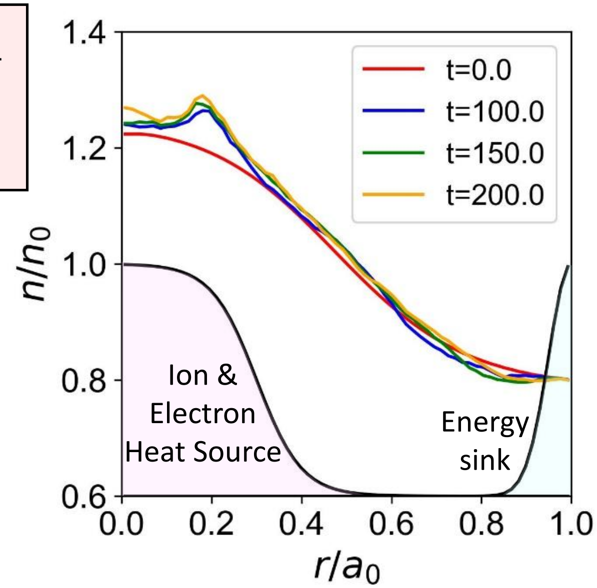

(B) Ion

$R_0/L_{T_i} = 10$

$R_0/L_{T_e} = 6$

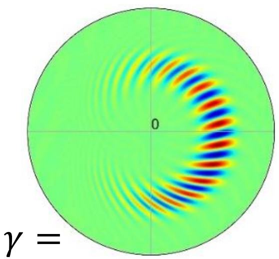

$\gamma =$ 0.71

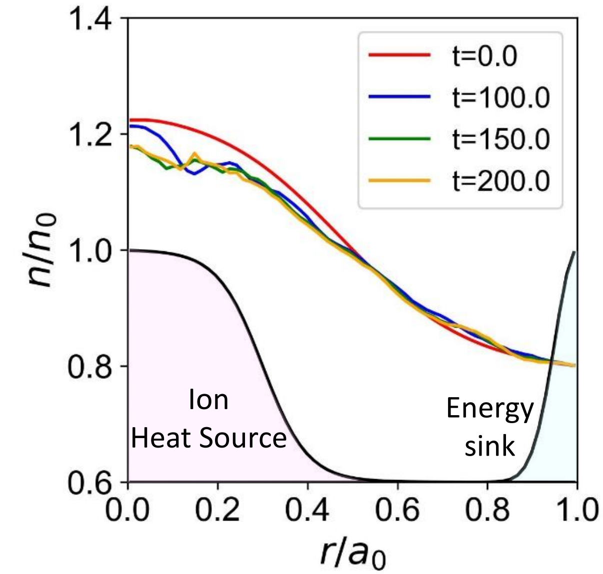

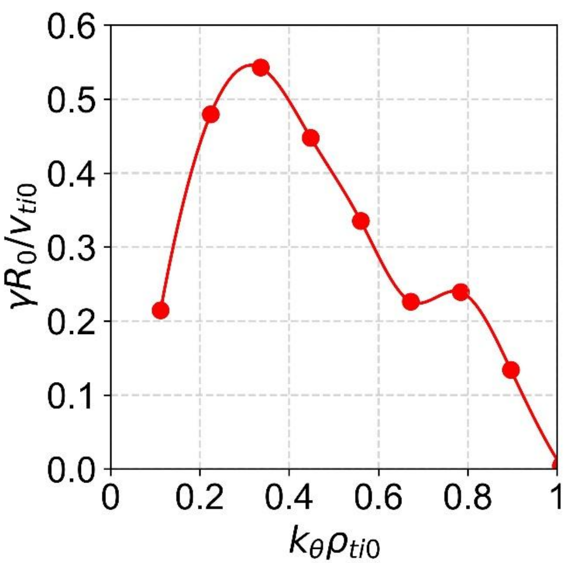

- ✓ ITG
  + weak TEM
- ✓ Ion/electron heating provides density peaking

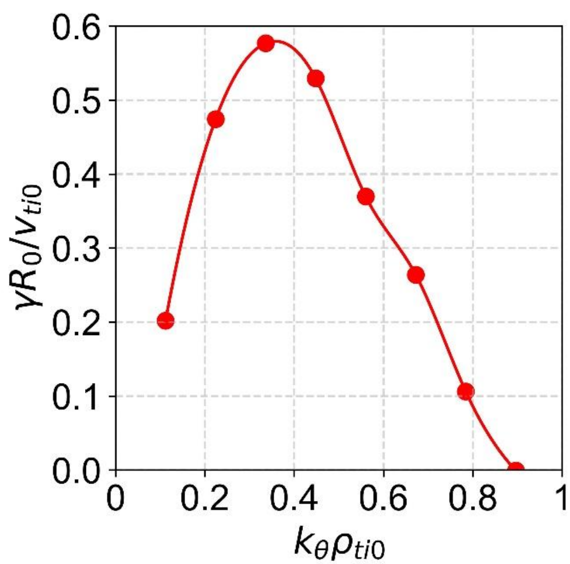

- ✓ Only ITG
- ✓ Ion heating provides density relaxation

(1) Summary of Turbulent Ion Particle Pinch

(A) Ion/Electron

$R_0/L_{T_i} = 10$

$R_0/L_{T_e} = 10$

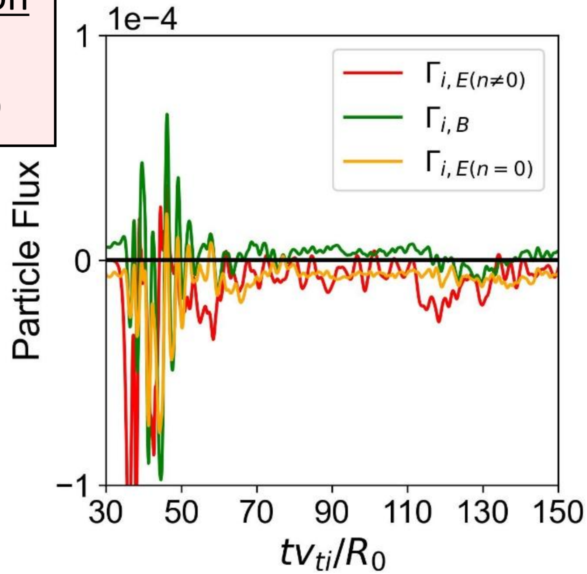

(B) Ion

$R_0/L_{T_i} = 10$

$R_0/L_{T_e} = 6$

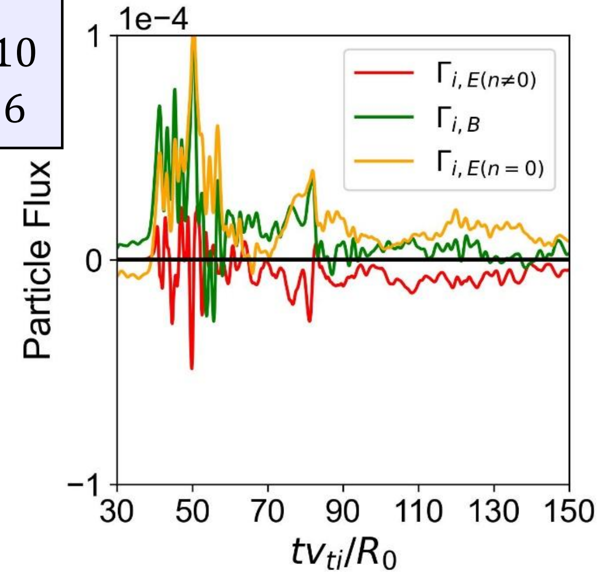

Step-1: Particle transport by E × B drift (n≠0) determined by temperature gradients

(A): $\Gamma_{i,E(n\neq0)} + \Gamma_{i,E(n=0)} + \Gamma_{i,B} - \Gamma_{e,E(n\neq0)} = 0$

- $\Gamma_{i,E(n\neq0)}$: Negative
- $-\Gamma_{e,E(n\neq0)}$: Strongly Positive

(B): $\Gamma_{i,E(n\neq0)} + \Gamma_{i,E(n=0)} + \Gamma_{i,B} - \Gamma_{e,E(n\neq0)} = 0$

- $\Gamma_{i,E(n\neq0)}$: Weakly Negative
- $-\Gamma_{e,E(n\neq0)}$: Negative

Step-2: Particle transport by E × B (n=0) and magnetic drift to satisfy the above balance

(A): $\Gamma_{i,E(n\neq0)} + \Gamma_{i,E(n=0)} + \Gamma_{i,B} - \Gamma_{e,E(n\neq0)} = 0$

- $\Gamma_{i,E(n\neq0)}$: Negative
- $\Gamma_{i,E(n=0)}$: Negative
- $\Gamma_{i,B}$: Weakly Negative
- $-\Gamma_{e,E(n\neq0)}$: Strongly Positive

(B): $\Gamma_{i,E(n\neq0)} + \Gamma_{i,E(n=0)} + \Gamma_{i,B} - \Gamma_{e,E(n\neq0)} = 0$

- $\Gamma_{i,E(n\neq0)}$: Weakly Negative
- $\Gamma_{i,E(n=0)}$: Positive
- $\Gamma_{i,B}$: Positive
- $-\Gamma_{e,E(n\neq0)}$: Negative

(2) Governing Equations and Parameters

Governing equations

GK Boltzmann(Vlasov) equation

$$\frac{\partial}{\partial t}(\mathcal{J} f_s) + \mathcal{J}\frac{d\boldsymbol{R}}{dt}\cdot\frac{\partial f_s}{\partial \boldsymbol{R}} + \mathcal{J}\frac{dv_\parallel}{dt}\frac{\partial f_s}{\partial v_\parallel} = \mathcal{J} C_{s,s}\ (s = i, e, He)$$

$$\frac{d\boldsymbol{R}}{dt} = \frac{1}{B^*_{\parallel,s}}\left[v_\parallel(\boldsymbol{\nabla}\times\boldsymbol{A}) + \frac{B_0}{\Omega_s}v_\parallel^2(\boldsymbol{\nabla}\times\boldsymbol{b}) + \frac{c}{e_s}H\,\boldsymbol{\nabla}\times\boldsymbol{b} - \frac{c}{e_s}\boldsymbol{\nabla}\times(H\boldsymbol{b})\right]$$

$$\frac{dv_\parallel}{dt} = -\frac{1}{m_s B^*_{\parallel,s}}\left[(\boldsymbol{\nabla}\times\boldsymbol{A})\cdot\boldsymbol{\nabla}H + \frac{B_0}{\Omega_s}v_\parallel\boldsymbol{\nabla}\cdot(H\boldsymbol{\nabla}\times b)\right]$$

\+

GK quasi-neutrality condition

$$\frac{1}{4\pi e_i}\nabla_\perp\cdot\frac{\rho_{ti}^2}{\lambda_{Di}^2}\nabla_\perp\phi + \iint\langle\delta f_i\rangle_{\alpha,i}\frac{B_\parallel^*}{m_i}dv_\parallel d\mu + \frac{1}{4\pi e_{He}}\nabla_\perp\cdot\frac{\rho_{tHe}^2}{\lambda_{DHe}^2}\nabla_\perp\phi + \iint\langle\delta f_{He}\rangle_{\alpha,He}\frac{B_\parallel^*}{m_{He}}dv_\parallel d\mu = \delta n_e$$

Parameters

Parameter	Value
a_0/ρ_i	100
a_0/R_0	0.36
$(R_0/L_n)_{r=a_0/2}$	2.22
$\sqrt{m_i/m_e}$	10
ν_i^*	0.025
ν_e^*	0.025

- ✓ 10% He is assumed
- ✓ Hereafter, we report the following two cases;

Case	R_0/L_{T_i}	R_0/L_{T_e}	Ion heating	Electron heating
(A) Ion/Electron	10	10	On	On
(B) Ion	10	6	On	Off

(2) Density Peaking/Flattening by Heating

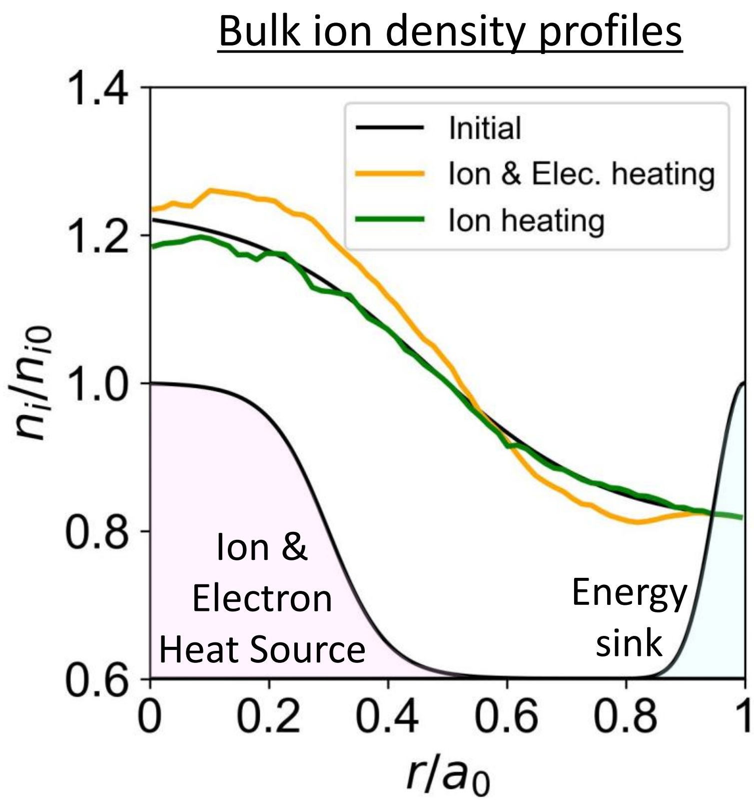

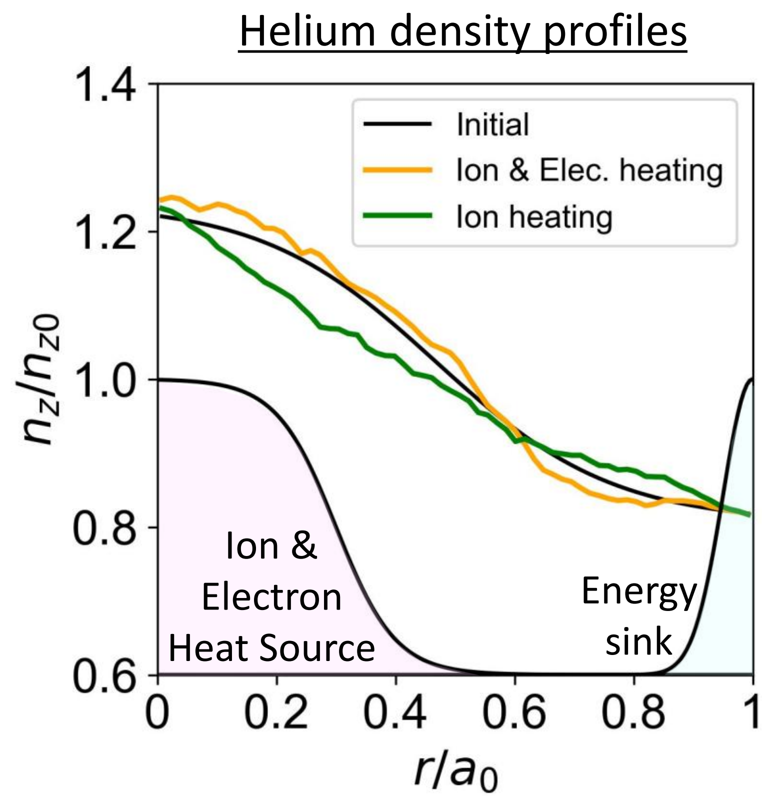

- ✓ Clear ion density peaking can be observed in the ion/electron heating case. But, Helium density is also slightly peaked.
- ✓ On the other hand, ion and helium density flattening weakly happens in the ion heating case.

(2) Ion & Helium Particle Flux

Particle fluxes in the ion/electron (left) and ion (right) heating cases

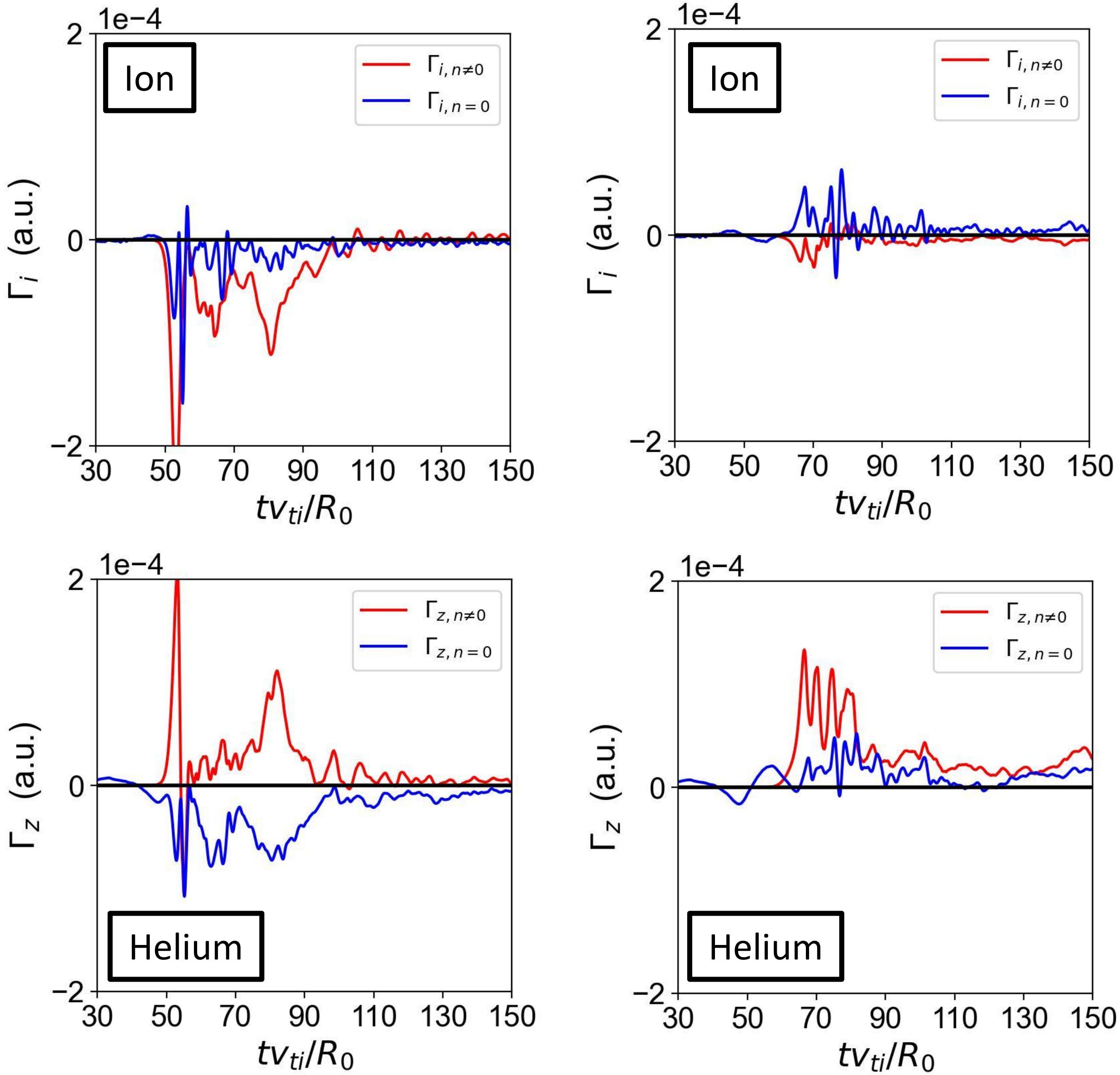

- ✓ Both ion particle pinches by non-axisymmetric and axisymmetric drifts are driven in the ion/electron heating case.
- ✓ On the other hand, He particle transport by non-axisymmetric and axisymmetric drifts cancel with each other.

(2) Effect of Non-Thermalized Helium

Bulk ion density profiles

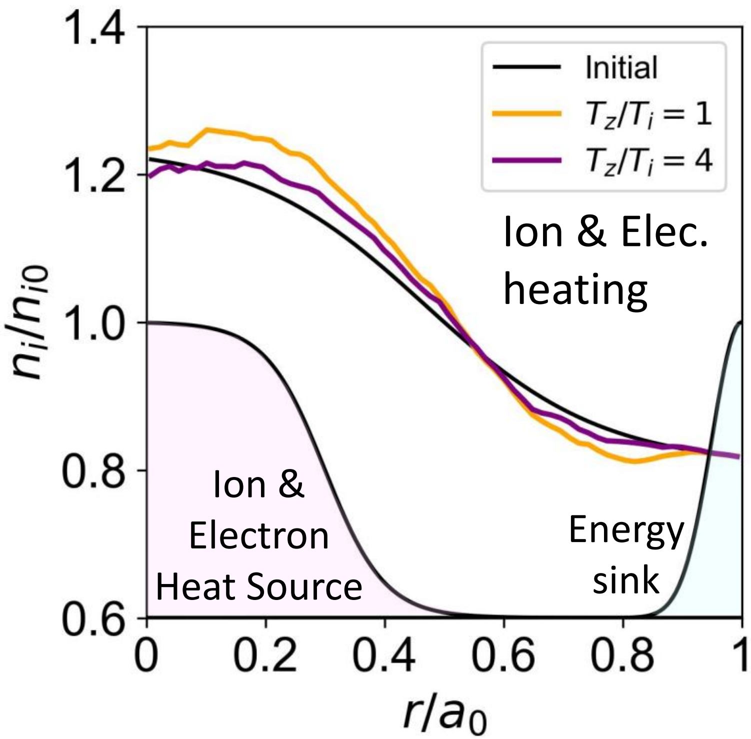

Helium density profiles

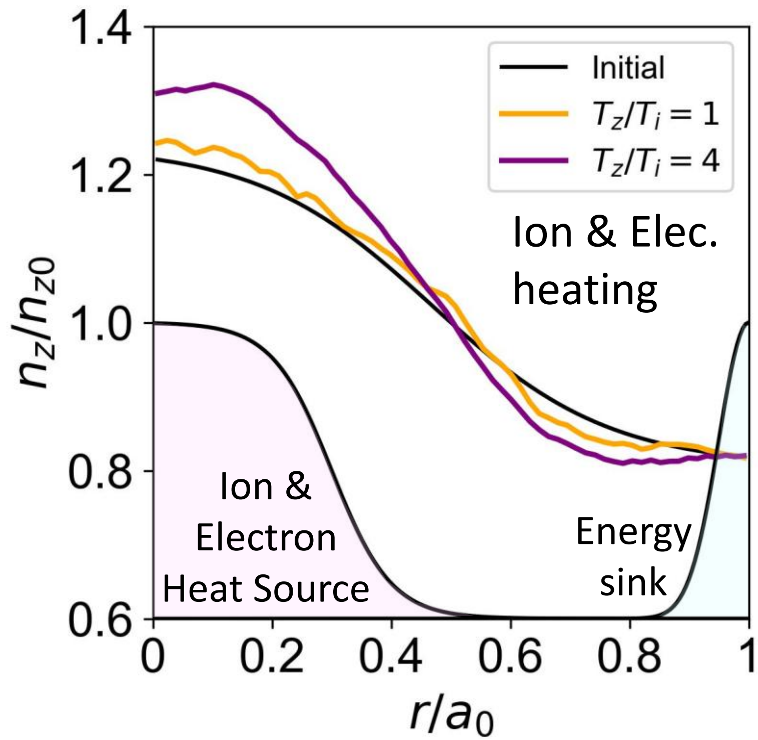

- ✓ When Helium temperature is higher than bulk ion one, it is newly found that ion particle pinch becomes weak and helium particle pinch is enhanced.
- ✓ It is reported that fast ions [P. Manas, NF-2020], ITG-TEM interactions [P. Palade, NF-2023], external torque [E. Fable, PPCF-2023] can change Helium particle transport, which will be checked as future works.

Contents

Introduction

Our new electromagnetic GKNET code with field aligned coordinate has achieved:

- ✓ Significant reduction in computational cost through the use of a field-aligned coordinate system
- ✓ Simulations with realistic tokamak equilibria via an interface coupled to an MHD equilibrium code

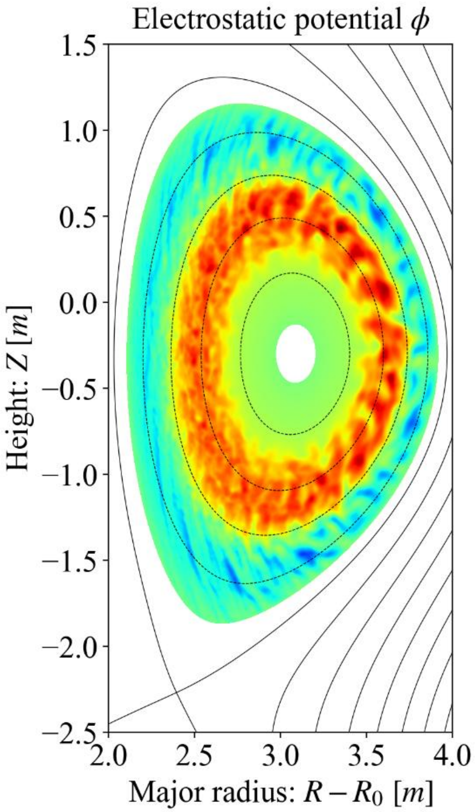

To validate the new code, linear benchmark comparisons were made with:

- ✓ **GENE** [Görler+, JCP-2011] : uses the same Eulerian method as GKNET
- ✓ **ORB5** [Lanti+, CPC-2020] : uses a different approach based on the Particle-In-Cell method

Field-aligned Coordinates

Field-aligned coordinates using the shifted metric technique

[Beer+, PoP-1995], [Scott, PoP-2001]

$$x = \rho \qquad [0,1]$$
$$y = y_{\mathrm{shift},j} - \zeta \qquad [0, 2\pi/N_w]$$
$$z = \theta - \theta_j \qquad [-\pi/N_s, \pi/N_s]$$

$$y_{\mathrm{shift},j} = \int_{\theta_j}^{\theta} \frac{\boldsymbol{B}\cdot\boldsymbol{\nabla}\zeta}{\boldsymbol{B}\cdot\boldsymbol{\nabla}\theta'} \mathrm{d}\theta' \quad (j = 0, 1, \ldots N_s - 1)$$

- ρ : Arbitrary radial label
- θ : Arbitrary poloidal angle label
- ζ : Geometrical toroidal angle
- N_s : Number of domain partitions
- N_w: Toroidal wedge number

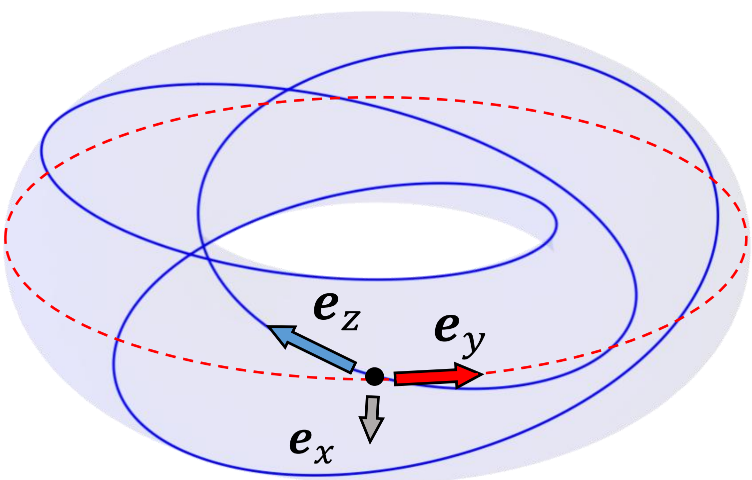

Covariant basis vectors
and a magnetic field line (blue)

- ✓ e_z is along the magnetic field line.
- ✓ Typical turbulent structures exhibit low wavenumbers along field lines, allowing for adequate resolution with fewer mesh points in the z-direction.
- ✓ In the electrostatic GKNET, this coordinate system requires lower computational cost by a factor of approximately 1/94. [Okuda+, PFR-2023]

Governing Equations

GK electromagnetic Vlasov equation

$$\frac{\partial \delta f_s}{\partial t} + \boldsymbol{V}_{\boldsymbol{R}}^{(0)} \cdot \nabla \delta f_s + \boldsymbol{V}_{\boldsymbol{R}}^{(1)} \cdot \nabla (f_{0s} + \delta f_s) + a_\parallel^{(0)} \frac{\partial \delta f_s}{\partial v_\parallel} + a_\parallel^{(1)} \frac{\partial}{\partial v_\parallel} (f_{0s} + \delta f_s) = 0$$

$$\boldsymbol{V}_{\boldsymbol{R}} = \frac{1}{B_{\parallel s}^*} \left[\boldsymbol{B}_0 v_\parallel + \frac{m_s}{q_s} v_\parallel^2 \nabla \times \boldsymbol{b}_0 + \frac{c}{q_s} \boldsymbol{b}_0 \times \nabla \left(\mu B_0 + q_s \langle \phi \rangle - q_s v_\parallel \langle A_\parallel \rangle \right) \right]$$

$$a_\parallel = - \frac{q_s}{m_s c} \frac{\partial \langle A_\parallel \rangle}{\partial t} - \frac{1}{m_s B_{\parallel s}^*} \left(\boldsymbol{B}_0 + \frac{m_s}{q_s} v_\parallel \nabla \times \boldsymbol{b}_0 - c \boldsymbol{b}_0 \times \nabla \langle A_\parallel \rangle \right) \cdot \nabla (\mu B_0 + q_s \langle \phi \rangle)$$

GK quasi-neutrality condition

$$\nabla_\perp \cdot \left(\frac{m_i n_{0i}}{B^2} \nabla_\perp \phi \right) = \sum_s \int q_s \delta f_s \mathrm{d}^3 \boldsymbol{v}$$

GK Ampère’s law

$$-\nabla_\perp^2 A_\parallel = \frac{4\pi}{c} \sum_s \int q_s v_\parallel \delta f_s \mathrm{d}^3 \boldsymbol{v}$$

GK induction equation (time derivative of Ampère’s law)

$$-\nabla_\perp^2 \frac{\partial A_\parallel}{\partial t} = \frac{4\pi}{c} \sum_s \int q_s v_\parallel \frac{\partial \delta f_s}{\partial t} \mathrm{d}^3 \boldsymbol{v}$$

Comparison with GENE code

- ✓ The linear benchmark with GENE is conducted using the parameters and simulation results presented in [Görler+, PoP-2016].
- ✓ The beta dependence of the eigenvalue at a fixed wavenumber is compared.

Parameters

Parameter	Value
a_0/ρ_i	180
a_0/R_0	0.36
$(R_0/L_T)_{r=a_0/2}$	6.96
$(R_0/L_n)_{r=a_0/2}$	2.23
m_i/m_e	1836
$q = 2.52\left(\frac{r}{a_0}\right)^2 - 0.16\left(\frac{r}{a_0}\right) + 0.86$	

- ✓ Concentric circular torus
- ✓ Only $n = 19$ mode is calculated using 1/19 wedge torus
- ✓ Realistic proton-electron mass ratio
- ✓ β_i values: 0–2.5% range tested
- ✓ $\beta_i \equiv 8\pi n_{i0} T_{i0} / B_{\mathrm{axis}}^2$ at $r = 0.5a_0$

Comparison with ORB5 code

- ✓ The linear benchmark with ORB5 is conducted using the parameters presented in [Mishchenko+, PPCF-2022].
- ✓ The beta dependence of the eigenvalue is compared across multiple wavenumbers.

Parameters

Parameter	Value
a_0/ρ_i	180
a_0/R_0	0.1
$(R_0/L_T)_{r=a_0/2}$	20
$(R_0/L_n)_{r=a_0/2}$	3
m_i/m_e	200
β_0	0.0952%
$q = \dfrac{0.8(r/a_0)^2 + 1.1}{\sqrt{1-(r/R_0)^2}}$	

- ✓ Concentric circular torus
- ✓ $\beta_i \equiv 8\pi n_{i0} T_{i0}/B_{\mathrm{axis}}^2$ at $r = 0.5a_0$
- ✓ β_i values: $\beta_0, 2\beta_0, 3\beta_0, 4\beta_0, 5\beta_0$

Contents

Summary & Future Plans for Topic-1

Summary

- ✓ A density peaking of bulk ion due to turbulent fluctuations can be achieved by sufficiently strong both ion and electron heating even in the presence of impurities.

$$\Gamma_{i,E\times B(n\neq 0)} + \Gamma_{i,E\times B(n=0)} + \Gamma_{i,B} - \Gamma_{e,E\times B(n\neq 0)} \cancel{- \Gamma_{e,E\times B(n=0)}} \cancel{- \Gamma_{e,B}} = 0$$

Negative by Ion heating ($\Gamma_{i,E\times B(n\neq 0)}$)

Negative to satisfy ambipolarity condition ($\Gamma_{i,E\times B(n=0)} + \Gamma_{i,B}$)

Positive by electron heating ($\Gamma_{e,E\times B(n\neq 0)}$)

Cancel with each other ($\Gamma_{e,E\times B(n=0)}$, $\Gamma_{e,B}$)

- ✓ Hot helium, i.e. higher T_{z0}/T_{i0} can prevent both fuel supply and helium ash exhaust, indicating the temperature ratio of helium to bulk ion is one of key parameters to control them.

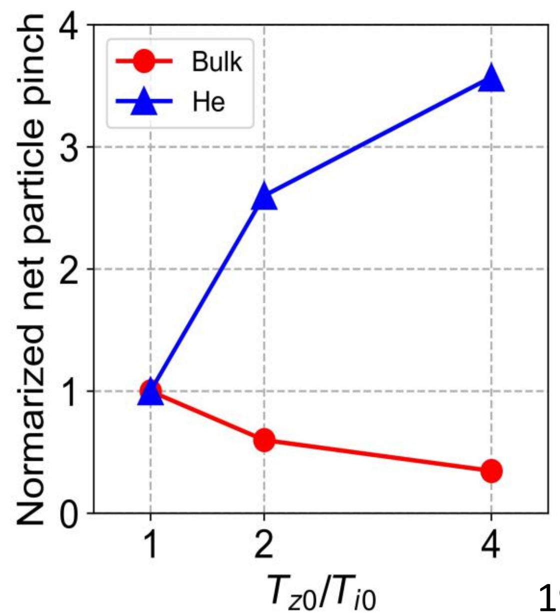

Future Plans

- ✓ Isotope effect
- ✓ Effect of temperature anisotropy
- ✓ Heating model

Summary & Future Plans for Topic-2

Summary

- ✓ Electromagnetic GKNET has been extended with field-aligned coordinates and an interface to MHD equilibrium codes.
- ✓ Linear benchmarks have shown good agreement between GKNET, GENE, and ORB5.

Future Plans

- ✓ Nonlinear simulation (already successful, further analysis needed)
- ✓ Beta dependence of shaping effects
- ✓ Micro tearing mode
- ✓ Energetic particle

Acknowledgment

We gratefully acknowledge Drs. Poli, Görler and Hayward-Schneider, Max-Planck-Institut für Plasmaphysik, for this work.